Development 128, 929-941 (2001)
Printed in Great Britain © The Company of Biologists Limited 2001
DEV3311

Rescuing desmoplakin function in extra-embryonic ectoderm reveals the importance of this protein in embryonic heart, neuroepithelium, skin and vasculature

G. Ian Gallicano*, Christoph Bauer and Elaine Fuchs‡

Howard Hughes Medical Institute, Department of Molecular Genetics and Cell Biology, The University of Chicago, Chicago, IL 60637, USA

*Present address: Department of Cell Biology, Georgetown University, Washington DC, USA

‡Author for correspondence (e-mail: lain@midway.uchicago.edu)

Accepted 21 December 2000; published on WWW 26 February 2001

SUMMARY

Desmosomes mediate intercellular adhesion through desmosomal cadherins, which interface with plakoglobin (PG) and desmoplakin (DP) to associate with the intermediate filament (IF) cytoskeleton. Desmosomes first assemble in the E3.5 mouse trophectoderm, concomitant with establishment of epithelial polarity and appearance of a blastocoel cavity. Increasing in size and number, desmosomes continue their prominence in extra-embryonic tissues, but as development proceeds, they also become abundant in a number of embryonic tissues, including heart muscle, epidermis and neuroepithelium. Previously, we explored the functional importance of desmosomes by ablating the *Dsp* gene. Homozygous *Dsp* mutant embryos progressed through implantation, but did not survive beyond E6.5, owing to a loss or instability of desmosomes and tissue integrity. We have now rescued the extra-embryonic tissues by aggregation of tetraploid (wild-type) and diploid (*Dsp* mutant) morulae. These animals survive several days longer, but die shortly after gastrulation, with major defects in the heart muscle, neuroepithelium and skin epithelium, all of which possess desmosomes, as well as the microvasculature, which does not. Interestingly, although wild-type endothelial cells of capillaries do not form desmosomes, they possess unusual intercellular junctions composed of DP, PG and VE-cadherin. The severity in phenotype and the breadth of defects in the *Dsp* mutant embryo is greater than PG mutant embryos, substantiating redundancy between PG and other armadillo proteins (e.g. β-catenin). The timing of lethality is similar to that of the VE-cadherin null embryo, suggesting that a participating cause of death may be a defect in vasculature, not reported for PG null embryos.

Key words: Desmosomes, Intercellular adhesion, Mouse, Desmoplakin, Plakoglobin

INTRODUCTION

Intercellular junctions play an important role not only in structuring the architecture of tissues, but also in integrating mechanical and signaling pathways (reviewed by Barth et al., 1997; Kowalczyk et al., 1999). Most adhering cells form classical adherens junctions, composed of the type of transmembrane receptor of the cadherin superfamily that associates with the actin cytoskeleton (for review, see Barth et al., 1997). However, during development of mammalian embryos, a number of tissues also rely upon a specialized type of calcium-dependent, intercellular adhesion mediated by the link of the intermediate filament (IF) cytoskeleton to other transmembrane receptors of the cadherin superfamily (Kowalczyk et al., 1999). While the precise role(s) of these connections remains undetermined, it has been surmised that the increased stability of the IF network over the actin cytoskeleton may help to provide greater stability to the types of intercellular connections that use this component of the cytoskeleton. This may be particularly important in tissues subjected to considerable mechanical stress, such as heart muscle, skin epidermis and some vascular endothelial structures, all of which feature cadherin-mediated connections to IFs.

The most common and robust of the intercellular junctions that use IFs are desmosomes, which are especially abundant in heart muscle and skin epidermis, but not seen in the vasculature. The desmosomal cadherins, desmogleins (Dsgs) and desmocollins (Dscs), form the transmembrane core of the desmosome (Koch and Franke, 1994; Kowalczyk et al., 1999). Specific vascular endothelial cells display unique intercellular junctions that are morphologically and biochemically distinct from either classical adherens junctions or desmosomes. These junctions, referred to as complexus adherens junctions or syndesmos, are composed of the endothelial-specific cadherin, VE-cadherin, rather than desmosomal cadherins (Schmelz and

Franke, 1993; Schmelz et al., 1994). VE-cadherin appears to interface with both actin and IF cytoskeletons (reviewed by Lampugnani and Dejana, 1997).

The extracellular domain of cadherins is responsible for calcium-dependent, homotypic interactions between cadherins on the surface of adjacent cells. The preference of a cadherin for a particular cytoskeletal network appears to be largely determined by its cytoplasmic domain, which can bind one or more of the armadillo family of cadherin-binding proteins. β-Catenin is the broadly expressed armadillo protein that binds preferentially to classical cadherins and to VE-cadherin (reviewed by Barth et al., 1997; Lampugnani and Dejana, 1997). Also broadly expressed, plakoglobin (PG) can bind classical cadherins and VE-cadherin (Cowin et al., 1986; Kowalczyk et al., 1998), but in cells that express desmosomal cadherins, it appears to have a strong preference for these family members (Kowalczyk et al., 1999). More restricted in their patterns of expression, plakophilin 1a associates with desmosomal cadherins in stratified and complex epithelia (McGrath et al., 1997), while plakophilin 2 plays a similar role in simple and complex epithelia (Mertens et al., 1996).

In contrast to β-catenin, which binds to α-catenin and links the classical cadherins to the actin cytoskeleton, PG and the plakophilins bind to desmoplakin (DP), a protein that interfaces with the IF cytoskeleton (reviewed by Barth et al., 1997; Kowalczyk et al., 1999). DP and PG are the only proteins expressed in all tissues, including heart muscle, neuroepithelium, skin epidermis and microvasculature, where intercellular junctions link to cytoplasmic IF networks (Kowalczyk et al., 1999 and references therein). These proteins are not typically found in classical adherens junctions, but they are components of desmosomes and complexus adherens junctions. DP is a large coiled-coil protein that has the capacity to associate with itself, with other desmosomal components and with IFs (Stappenbeck and Green, 1992; Stappenbeck et al., 1993; Kouklis et al., 1994; Kowalczyk et al., 1997; Smith and Fuchs, 1998). Through its C-terminal segment, DP directly binds to IFs, suggesting its indispensability for junctions that require this attachment (Kouklis et al., 1994; Kowalczyk et al., 1997).

The physiological roles of PG and DP in complexus adherens junctions are still unclear. Recently, it has been shown that when artificially expressed in mouse fibroblasts in vitro, VE-cadherin can recruit DP to cell-cell borders, but the process requires PG, and cannot be substituted for by its cousin β-catenin (Kowalczyk et al., 1998). In vivo, however, no defect in microvasculature has been reported in the PG-null embryo (Ruiz et al., 1996; Bierkamp et al., 1996). Moreover, most PG-null embryos die of heart failure from E10.5-12.5 onwards, in contrast to VE-cadherin mutant embryos, which die of vasculature defects by E9.5 (Carmeliet et al., 1999). On some genetic backgrounds, PG-null mice survive to birth, and exhibit skin blistering and heart abnormalities but, again, no overt defects in vasculature (Bierkamp et al., 1999). As β-catenin may be able to partially but not totally compensate for PG at desmosomes (Bierkamp et al., 1999), it remains undetermined how important this protein and desmosomes might be in cardiac and skin development, let alone in tissues that possess complexus adherens junctions.

The role of DP in any somatic tissue remains unaddressed. While the *Dsp* gene was successfully targeted for ablation in the mouse genome, the protein has no compensatory counterpart. Consequently, *Dsp* mutant embryos die very early (E5.5-6.5) most likely owing to defects in the extra-embryonic tissues (visceral endoderm, extra-embryonic ectoderm and trophectoderm) (Gallicano et al., 1998). These extra-embryonic defects cause a subsequent failure of the expansion of the egg cylinder of the developing mouse embryo (Gallicano et al., 1998).

The tissue instabilities observed in the extra-embryonic tissues of *Dsp* null embryos and in the heart muscle of PG null embryos correlate with a reduction in the number, size and structure of desmosomes in these tissues (Bierkamp et al., 1996; Gallicano et al., 1998). However, the requirement for desmosomes in extra-embryonic tissues coupled with the partial redundancy of PG with its cousins has precluded elucidation of the roles of embryonic desmosomes, which appear at gastrulation at E7.5 (Jackson et al., 1981; Schwarz et al., 1995), or for embryonic complexus adherens junctions, which appear during vasculogenesis at E8.5-E9.5 (Drake and Fleming, 2000).

To begin to explore the functional significance of desmosomes and complexus adherens junctions in embryonic development, we have used the tetraploid aggregation approach to rescue the lethal phenotype in $Dsp^{-/-}$ extra-embryonic ectoderm. This has enabled us for the first time to analyze DP function in developing somatic tissues. Interestingly, we find that DP null embryos supported by wild-type extra-embryonic tissues still exhibit defects that appear to be significantly more severe than those of PG mutant embryos. Most importantly, while DP null embryos were partially rescued up to E10 of embryonic development, they displayed marked abnormalities, not only in desmosome-containing tissues, such as heart muscle, neuroepithelium and skin epidermis, but also in complexus adherens junction-containing tissues, such as microvasculature.

MATERIALS AND METHODS

Production of $Dsp^{-/-}$ embryos by tetraploid aggregation

CD-1 female mice were superovulated and mated (Gallicano and Capco, 1995). After approximately 1.5 days, two-cell embryos were flushed from oviducts, collected in FMC media (Specialty Media, Phillipsburg, NJ), and equilibrated in fusion medium (0.3 M mannitol, 0.1 mM MgSO4, 50 mM CaCl2, 3% w/v bovine serum albumin; Duncan et al., 1997) for at least 5 minutes. Using a pulled, cotton-plugged glass pipette and mouth pipet aid, embryos were placed between electrodes submersed in fusion medium in a 100mm petri dish (BTX, Genetronix, San Jose, CA). They were aligned in a 0.6V alternating current field and pulsed with a single 125 μseconds direct current pulse of 110V. The embryos were transferred to a small drop of KSOM media (Specialty Media, Phillipsburg, NJ), covered with mineral oil and incubated for 30-45 minutes at 37°C to allow fusion of the two-cell embryos into a single-cell tetraploid embryo. Fused embryos were isolated and cultured overnight.

$Dsp^{+/-}$ female mice in a C57Bl6 genetic background were superovulated and mated with $Dsp^{+/-}$ males at the same time as the superovulated CD-1 females were mated (see above). Two-cell diploid embryos were removed from oviducts, placed in droplets of KSOM media, and incubated overnight so as to synchronize staging of diploid

and tetraploid embryos. The next afternoon, acid Tyrodes solution (pH 2.5) (Hogan et al., 1994) was used to remove the zona pellucidas from all embryos (diploid and tetraploid) that had proceeded to the four- to eight-cell stage. Using these embryos for aggregation, two tetraploid embryos were placed into a KSOM-filled depression that was made by a darning needle. One diploid embryo was added to each depression containing two tetraploid embryos making a sandwich of embryos (tetraploid/diploid/tetraploid; Nagy et al., 1993). Alternatively, *Dsp*$^{-/-}$ embryonic stem (ES) cells (see below) were added to the depression instead of diploid embryos. After 24-36 hours of incubation, successful aggregates formed blastocysts that were then transferred to the uterine horns of foster CD-1 females. Recipients were sacrificed at E6.5, E9.5, E10.5 and E12.5 for analysis of embryonic and extra-embryonic tissues.

Production of *Dsp*$^{-/-}$ ES cells

The procedure of Mortensen et al. was used to produce homozygous null *Dsp* ES cells (Mortensen et al., 1992). Briefly, 129/Sv ES cells heterozygous for the *Dsp* gene were plated at 5×10^5 cells per 100mm dish, followed by selection with either 1.5mg/ml or 2.0mg/ml G418 for 10- 14 days. Colonies that survived and appeared undifferentiated were genotyped by PCR and southern blot. Two clones had inactivated both *Dsp* genes, and were used for subsequent study.

Differentiation of embryoid bodies (EBs)

Specific endothelial differentiation of EBs was performed following the procedure of Vittet et al. (Vittet et al., 1996; Vittet et al., 1997). *Dsp*$^{+/+}$, *Dsp*$^{+/-}$ and *Dsp*$^{-/-}$ EBs were grown in IMDM Glutamax media (GIBCO, Rockville, MD) supplemented with 1.0% w/v methylcellulose (methocel MC, high viscosity; Fluka), 15% v/v fetal calf serum, 450 μM monothioglycerol, 10 μg/ml insulin (Boehringer), 50 units/ml penicillin, 50 μg/ml streptomycin, 50 ng/ml vascular endothelial growth factor (VEGF) (Peprotech, Rocky Hill, NJ), 100 ng/ml fibroblast growth factor 2 (Peprotech) and 10 ng/ml murine interleukin 6 (Peprotech). ES cells were seeded between 1.25×10^3 and 2.5×10^3 cells/ml in a final volume of 2 ml in 35 mm petri dishes. EBs were analyzed for vascular formation by immunohistochemistry, immunofluorescence or western blot after 14 days of incubation in either supplemented media (above), media containing leukemia inhibitory factor (LIF) (undifferentiated), or media without LIF (differentiated along a different pathway than endothelial).

Analysis of genotype by PCR

Genomic DNA was prepared from embryo tails by incubation in Gittsuhier buffer and 0.1 mg/ml proteinase K at 55°C overnight (Hogan et al., 1994). PCR was performed on lysates after inactivating proteinase K at 96°C for 10 minutes and centrifugation. Three primers (see Gallicano et al., 1998 for sequences) were used in a 25 μl PCR reaction that cycled 42 times, beginning at 94°C for 30 seconds, followed by 56°C for 30 seconds and ending at 72°C for 30 seconds. PCR amplification of the mutant allele resulted in a 300 bp product while the amplification of the wild type allele resulted in a 220 bp product.

Embryo histology, immunohistochemistry and confocal microscopy

Embryos were prepared for either paraffin sectioning for best tissue preservation or frozen sectioning for confocal microscopy. For paraffin embedding, embryos were fixed in 4% paraformaldehyde, prepared for sectioning as described by Kaufman (Kaufman, 1992), and stained with Hematoxylin and Eosin. Some paraffin sections were subjected to immunohistochemistry following the Vectastain (Novocastra, CA) protocol. Primary antibodies to either DP 2.15, a mouse monoclonal against the rod/tail of DP (5 μg/ml; ICN Biochemicals, Costa Mesa, CA), E-cadherin (Zymed, San Francisco, CA), rabbit anti-plakoglobin (anti-PG; 1:100, a gift from Dr Jackie Papkoff, Megabios Corp. Burlinggame, CA) or anti-pan DSG (Transduction Labs, Inc.) were used followed by incubation in secondary antibodies conjugated to biotin. After a final incubation in an avidin conjugated to horse radish peroxidase, color detection was developed using Vectastain Nova Red color enhancement kit. All immunolabeling was performed using the Mouse on Mouse (M.O.M.) kit (Vectastain) to minimize background.

Embryos were analyzed for confocal microscopy by freezing the entire decidua in OCT compound, sectioning (10 μm) and analysis by indirect immunofluorescence (for protocol, see Gallicano et al., 1998). Antibodies used for this assay included those listed above as well as three affinity-purified rabbit polyclonal anti-DP antibodies directed against either the tail (1:50 Gallicano et al., 1998), rod (1:100; Kouklis et al., 1994; Gallicano et al., 1998) or head domain (1:10; Smith and Fuchs, 1998; Gallicano et al., 1998). Analysis of sections after incubation in appropriate primary and secondary antibody conjugated to either Texas Red or FITC were performed using a Carl Zeiss 410 confocal microscope (Thornwood, NY).

HRP uptake assay

E6.0 embryos from *Dsp*$^{+/-}$ crosses were carefully isolated from their decidua, incubated for 1 hour in 50% rat serum, 25% mouse serum, and 25% Dulbecco's modified Eagle medium at 37%C, and then incubated in the same media containing 2 mg/ml horseradish peroxidase (HRP) for 30 minutes at 37°C. Embryos were washed in media free of HRP, fixed and processed as described in Kadokawa et al. (Kadokawa et al., 1987). Embryos then were processed for paraffin embedding, sectioned onto glass slides, and photographed. Wild-type and mutant embryos were resolved three ways: morphologically, using a dissecting microscope, by subjecting serial sections of each embryo to anti-DP antibodies; or by isolating and subjecting embryonic ectoderm to PCR using primers recognizing mutant or wild-type alleles (see above).

Cell proliferation and apoptosis assays

For cell proliferation, cells in S phase of the cell cycle were labeled with bromodeoxyuridine (BrdU) (Boehringer, Mannheim, Germany). BrdU (100 μg/gram of body weight) was injected intraperitoneally into pregnant females either 5-6.5 or 9.5 days post-coitum. Females were sacrificed 30-40 min after injection, and, taking extreme care, embryos were isolated from their decidua. After fixation in 4% paraformaldehyde for 1 hour at room temperature, embryos were permeabilized with 0.5% Triton X-100 in blocking buffer for 1 hour at room temperature. Embryos were then incubated in blocking buffer containing anti-BrdU (Boehringer) for 1-2 hours and visualized with the appropriate secondary antibody conjugated to Alexa-594 secondary antibody (Molecular Probes, Inc., Eugene OR). DAPI was used as a nuclear marker. All positive (red) nuclei were counted in each tissue type the ratio of labeled to total nuclei per confocal section was quantified and graphed. The genotype of each embryo was determined by double labeling with anti-DP followed by FITC labeled secondary antibody. Four mutant and four wild-type embryos were analyzed in the study.

To assay for apoptosis, the TUNEL reaction, which detects incorporation of biotinylated dUTP carried out by terminal transferase, was used on whole-mount embryos that were carefully isolated from their deciduas (E5.5-E6.5) or yolk sac (E9.5-E10). Intact embryos (E5-E6) or sections (E10) were subjected to the ApopTag in situ apoptosis detection protocol (Oncor, Gaithersburg, MD), which was modified for handling smaller embryos. Microdrops of each solution were placed into 35 mm petri dishes and embryos were transferred into each drop for the times specified by the protocol. Quantification of all positive TUNEL nuclei was performed using confocal microscopy.

RESULTS

Defects in extra-embryonic tissues have an impact on DP null mutant embryo development, even though DP is not expressed in the embryo proper prior to gastrulation

Previously, we reported the generation of *Dsp*$^{-/-}$ mutant embryos and their marked defect in desmosome formation in extra-embryonic tissues (Gallicano et al., 1998). *Dsp*$^{-/-}$ embryos die by E6.0-E6.5, owing to dissociation of extra-embryonic tissues (ectoplacental cone, EPC; extra-embryonic ectoderm, EXE; visceral endoderm, VE; and parietal endoderm, PE), which are all rich in desmosomes; this in turn causes a failure of egg cylinder formation within the embryonic ectoderm (ECT), which adheres only through classical adherens junctions and not desmosomes (compare Fig. 1A with Fig. 1B; Gallicano et al., 1998). Based upon these data, we surmised that lethality of the embryo proper was likely to be a secondary defect elicited by the abnormalities in extra-embryonic tissues. We have since explored in greater detail the differences between extra-embryonic and embryonic tissues in the *Dsp*$^{-/-}$ null embryos. First, we assessed whether cellular proliferation may have been affected in the developing E5.0 and E6.0 *Dsp*$^{-/-}$ mutant embryos. As judged by BrdU labeling, E6.0 DP null embryos exhibited a significant decrease in proliferation (up to approx. fourfold) in all tissues, including embryonic as well as extra-embryonic (Fig. 1C-E). In contrast, at E5.0 only a twofold decrease was detected, and this was primarily in extra-embryonic tissues (Fig. 1C). The reduction in proliferation seen in *Dsp*$^{-/-}$ mutant embryos could not be attributed to a concomitant increase in apoptosis, as no significant differences were detected in the percentage of TUNEL-positive cells in extra-embryonic or embryonic tissues of wild-type versus *Dsp* mutant embryos (Fig. 1F-H). Taken together, these data suggest that the proliferative defect in E6.0 *Dsp* mutant embryonic ectoderm is likely to be a secondary consequence of primary defects in extra-embryonic tissues.

Supporting our findings is the earlier work of Duncan et al., who discovered that extra-embryonic visceral endoderm plays a critical role in defining the environment necessary for the ectodermal growth prior to and during gastrulation (Duncan et al., 1997). Visceral endoderm may function in large part by excluding the entry of unwanted components into the ectoderm (reviewed by Jollie, 1990). To determine more precisely if the

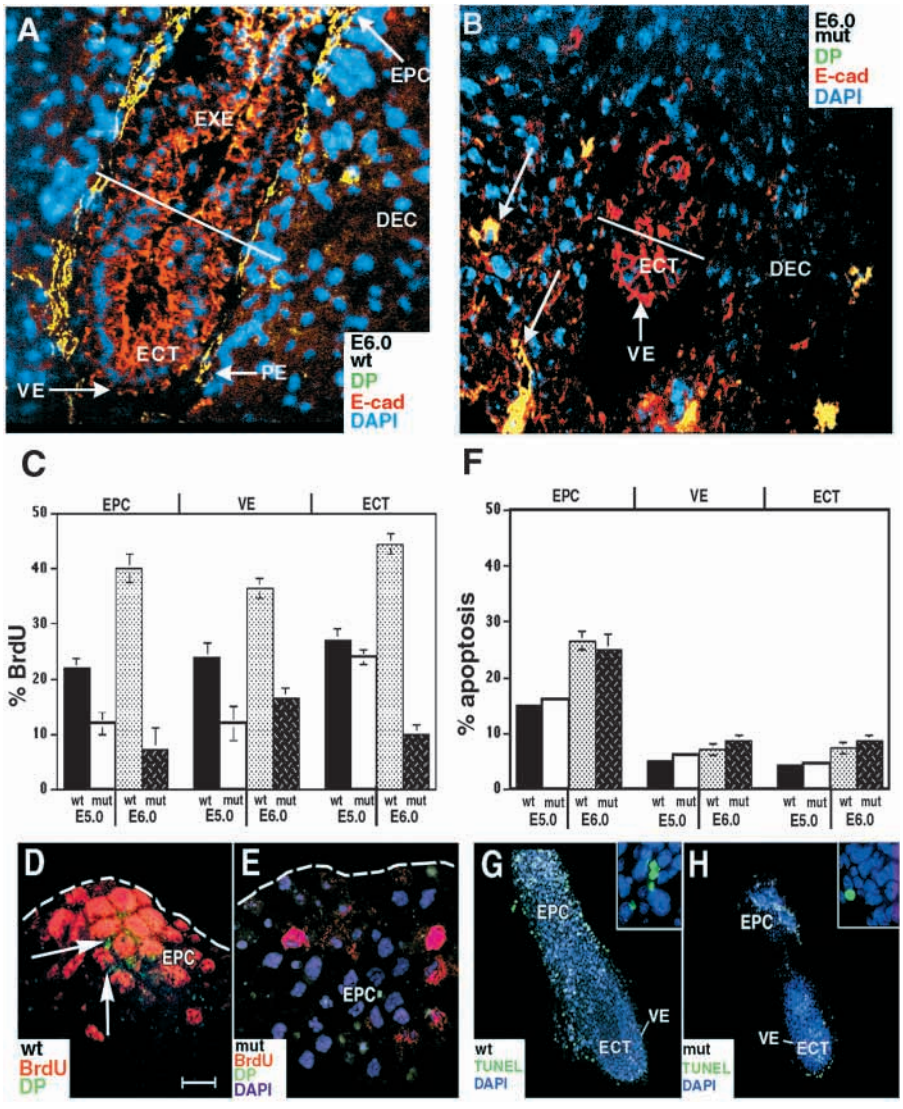

Fig. 1. *Dsp* expression in wild-type and mutant embryos. (A,B) Frozen sections of a wild-type (A) and *Dsp*$^{-/-}$ (B) E6.0 embryos surrounded by maternal deciduas. Embryos were stained with antibodies directed against DP (green) and E-cadherin (red). Maternal decidual crypts acted as built-in controls for DP staining in mutant embryos (arrows in B). White line demarcates boundary between extra-embryonic ectoderm (above) and embryonic ectoderm (below). (C-E) BrdU incorporation in E5.0 and E6.0 embryos. Anti-BrdU-labeled nuclei were detected with a Texas Red secondary antibody. Graph shows percentage of nuclei labeled within each tissue. Note that by E6.0, proliferation was significantly decreased in most *Dsp*$^{-/-}$ tissues. (D,E) Representative confocal views of E6.0 EPC showing nuclei staining positive for BrdU (red). Anti-DP antibodies followed by secondary antibodies conjugated to FITC were used to identify wild-type and mutant embryos. DP (green) is localized at wild-type cell-cell junctions (arrows in D). (F-H) TUNEL assays were used to identify apoptotic nuclei. TUNEL-positive nuclei (green) were counted in each embryonic tissue and graphed as percentages of total nuclei. No significant difference in the percentage of TUNEL-positive nuclei was detected at either E5.0 or E6.0, although embryo size was considerably reduced in E6.0 mutant embryos. (G,H) Representative examples; insets at higher magnification. DEC, decidua; ECT, embryonic ectoderm; EPC, ectoplacental cone; EXE, extra-embryonic ectoderm; PE, parietal endoderm; VE, visceral endoderm. Scale bar: 10 μm in A,B; 30 μm in D,E; 75 μm in G,H.

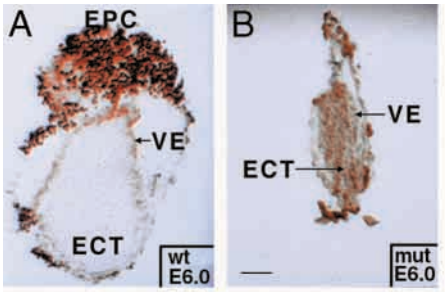

Fig. 2. HRP uptake assay to test functional competency of visceral endoderm. After the HRP uptake assay (see Materials and Methods), E6.0 embryos were frozen and sectioned. HRP uptake in VE and EPC, but not in ECT indicates that VE is functioning properly in wild-type (A) but not in *Dsp*$^{-/-}$ (B) embryos. Scale bar: 75 μm.

visceral endoderm malfunctions in *Dsp* mutant embryos, E6.0 *Dsp* mutant and wild-type embryos were carefully isolated from their deciduas and incubated in media containing horse radish peroxidase (HRP). Fixation and staining with diaminobenzidine revealed that in wild-type embryos, a fully functional visceral endoderm can endocytose HRP, but does not allow it to enter the ectodermal compartment (Fig. 2A; Kadokawa et al., 1987). In contrast, the *Dsp*$^{-/-}$ embryos failed to exclude HRP from the ectoderm (Fig. 2B). Taken together, embryonic lethality in *Dsp*$^{-/-}$ mutant embryos was most likely caused at least in part by a failure of the visceral endoderm to filter out components from the maternal environment.

Dsp$^{-/-}$ embryos progress through gastrulation when supplemented with *Dsp*$^{+/+}$ extra-embryonic tissues

If lethality in *Dsp*$^{-/-}$ embryos is caused by a failure of the visceral endoderm, then rescuing the lethal phenotype should be possible by supplementing *Dsp*$^{-/-}$ embryos with wild-type extra-embryonic tissue. This approach is feasible through a technique known as tetraploid rescue, in which diploid cells from *Dsp*$^{-/-}$ C57Bl6 mouse embryos or *Dsp*$^{-/-}$ 129/Sv mouse ES cells (or their wild-type counterparts as controls) are aggregated with tetraploid cells engineered from wild-type embryos (Fig. 3A). When chimeric aggregates are cultured to the blastocyst stage and then allowed to develop further in foster mothers, embryonic tissue derives solely from the diploid portion of the aggregate, while the extra-embryonic tissue is completely tetraploid (Nagy et al., 1993; Dragatsis et al., 1998; Kupriyanov and Baribault, 1998). We refer to the tetraploid aggregation with wild-type contol or *Dsp*$^{-/-}$ cells as 'wild-type rescue' or 'mutant rescue', respectively (wt resc, mut resc).

At the equivalent of E7.5, wild-type and mutant 'rescued' embryos derived from chimeric blastocysts appeared indistinguishable from unmanipulated, normal E7.5 embryos (Fig. 3B,C). In contrast, rescued *Dsp* mutant embryos harvested shortly thereafter, began to exhibit marked phenotypic abnormalities, and by E10, the *Dsp* mutant embryos were extremely small and malformed relative to their control counterparts (Fig. 3D,E). Out of 25 foster mothers harboring chimeric embryos, five contained a *Dsp* mutant E10 embryo with a phenotype similar to the example shown. These mutant embryos were still alive, as evidenced by their heart, which was still beating, albeit extremely slowly (approx. five

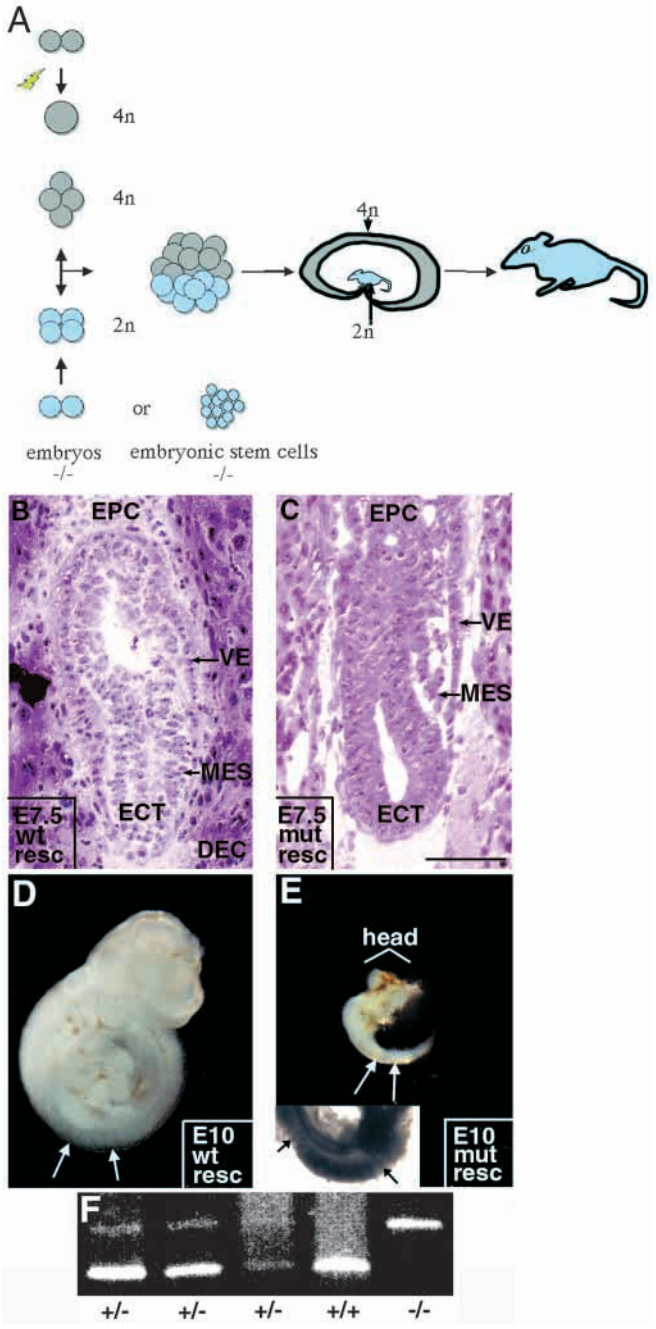

Fig. 3. Pregastrulation lethality (E6.5) is rescuable by tetraploid aggregation. (A) General principle of the tetraploid aggregation experiment (see Materials and Methods). (B,C) E7.5 embryos derived from wild-type and *Dsp*$^{-/-}$ tetraploid aggregates. Embryos were fixed, embedded and stained with Hematoxylin and Eosin. MES, mesoderm. (D,E) E10 'rescued' embryos derived as above. Arrows point to somites (inset to E shows higher magnification). (F) Genotyping of 'rescued' E10 embryos. Three embryos were heterozygous; the embryo in D was homozygous wild type (second to last lane) and the embryo in E was *Dsp*$^{-/-}$ (far right-hand lane). Scale bar: 100 μm for B,C; 2 mm for D,E.

beats per minute) relative to wild-type embryos (75-80 beats per minute). This caused the blood to exit from the heart tube at a considerably slower rate, and signs of hemorrhaging were visible. Despite the obvious defects, the development of

Dsp$^{-/-}$-rescued embryos progressed considerably further than DP null embryos (Gallicano et al., 1998): in contrast to the null embryos, the *Dsp*$^{-/-}$-rescued embryos underwent gastrulation and formed mesodermal components such as somites (arrows in Fig. 3E and in inset).

The genotype of the embryos from each litter was confirmed by PCR (Fig. 3F) and by staining with anti-DP antibodies (see below). By E12.5, no *Dsp*$^{-/-}$ embryos were found in any of the litters from five foster mothers that harbored chimeric embryos. This finding suggests that by this time most, if not all, the *Dsp*$^{-/-}$ embryos had died and were resorbed in the womb.

Histological analyses of rescued *Dsp*$^{-/-}$ embryos show severe defects in tissues that normally possess desmosomes, including heart muscle, neuroepithelium and skin epidermis

To analyze the *Dsp* mutant phenotype further, E10 *Dsp*$^{-/-}$ embryos were embedded in paraffin, sectioned and stained with Hematoxylin and Eosin. A sagittal section through a wild-type embryo confirmed that morphogenesis of specific organs was well underway (Fig. 4A). A well-formed heart (ht) was visible as was the neuroepithelium (ne) comprising the headfolds of the developing brain and the spinal canal (sp). In the mutant embryo, heart tissue was visible, but the overall architecture of the heart was severely deformed (Fig. 4B). Neuroepithelium also was present; however, in all sections from *Dsp*$^{-/-}$ embryos, a common phenotype was the lack of well-formed headfolds and a properly developed spinal canal (Fig. 4B).

Higher magnification of cardiac tissue revealed a distinct blood filled lumen (lu) surrounded by endocardium (endo), myocardium (myo) and epicardium (epi) (Fig. 5A). In contrast, sections from *Dsp*$^{-/-}$ embryos revealed a misshapen, partially collapsed heart (Fig. 5B). Interestingly, despite this partial collapse of the organ, all three tissues of the heart were still evident and the heart was able to beat and push blood. These data suggest that proliferation, differentiation and overall heart structure were not dependent upon DP (Fig. 5B).

The appearance of desmosome-like structures in the intercalated disks and the onset of expression of desmosomal components in the developing heart begins shortly after gastrulation (van der Loop et al., 1995). By E10, DP expression was readily detected in the wild-type epicardium, myocardium and endocardium (Fig. 5C). Anti-DP antibodies never stained DP null embryos (Fig. 5D). Antibodies against other desmosomal-specific markers, such as desmoglein 2 (Dsg2),

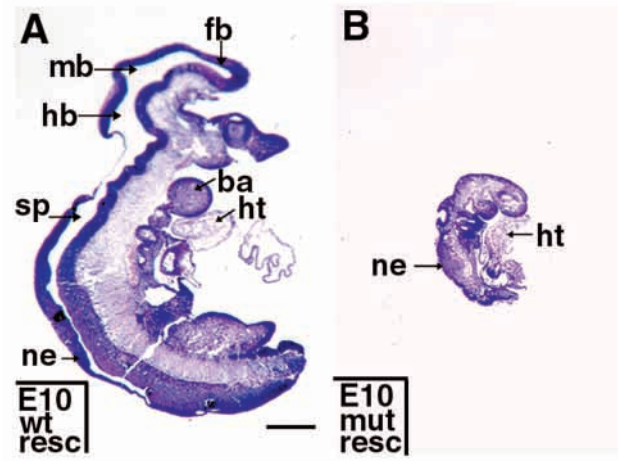

Fig. 4. Histology of wild-type and *Dsp*$^{-/-}$ E10 embryos. Embryos were paraffin embedded, sectioned sagittally and stained with Hematoxylin and Eosin. Embryos were photographed at same magnification. Note smaller size and defective heart and neural tube development in *Dsp*$^{-/-}$ embryo. ba, branchial arch; fb, forebrain; hb, hinbrain; ht, heart; mb, midbrain; ne, neurectoderm; sp, spinal chord. Scale bar: 0.5 mm.

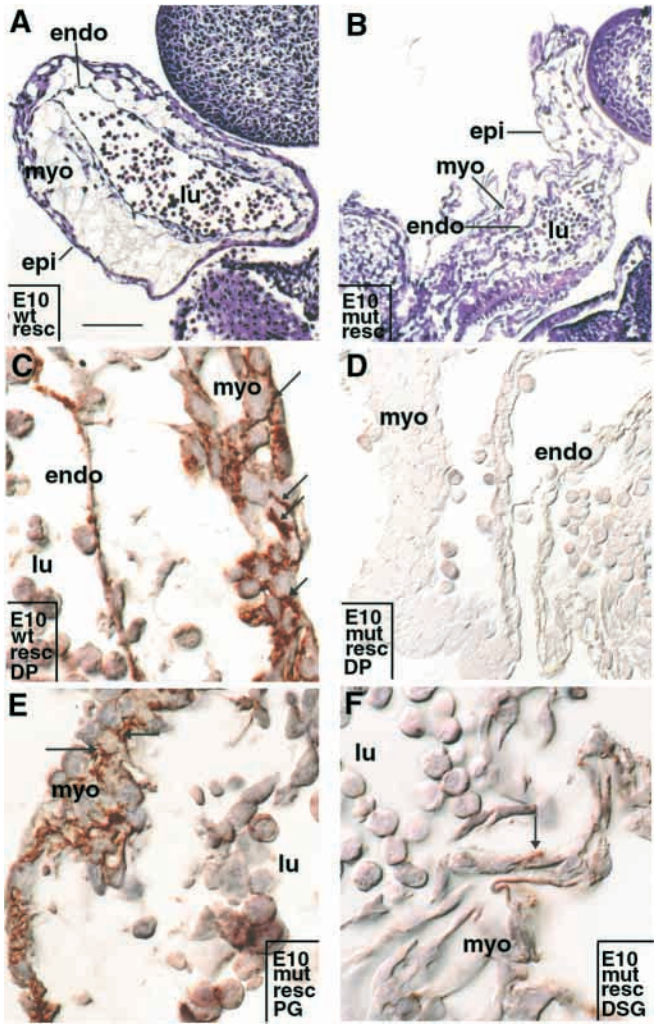

Fig. 5. Histology and immunohistochemistry of cardiac development in E10 wild-type and *Dsp*$^{-/-}$ embryos. (A) Hematoxylin and Eosin staining of wild-type heart shows a blood-filled lumen surrounded by endocardium (endo), myocardium (myo) and epicardium (epi). (B) Hematoxylin and Eosin-stained section of a heart from a *Dsp*$^{-/-}$ embryo shows a small blood-filled lumen surrounded by normal-looking endo, myo and epicardium; however, cardiac morphology appears flattened or partially collapsed. (C) High magnification view of wild-type heart stained with antibodies to DP followed by HRP enhancement (brown) shows anti-DP staining at cell junctions (arrows). (D) No DP staining was present in *Dsp*$^{-/-}$ heart. (E) Arrows point to staining of anti-plakoglobin (PG) at cell junctions in myocardium from a *Dsp*$^{-/-}$ embryo. (F) Only a few cell junctions stained with antibodies against desmoglein (arrow). lu, lumen. Scale bar: 100 μm in A,B; 35 μm in C,E,F; 50 μm in D.

still stained the tissue, but staining was significantly decreased over wild type (Fig. 5F). In contrast, staining appeared largely unaffected with antibodies against PG, a protein that localizes to adherens junctions as well as desmosomes (Fig. 5E).

Taken together, these results extended our earlier findings, where we discovered that in the absence of DP, extra-embryonic tissues show a reduction in desmosomes without apparent loss of adherens junctions (Gallicano et al., 1998). Despite comparable genetic backgrounds, the heart defects caused by the lack of DP were significantly more severe to those seen when PG was missing (Ruiz et al., 1996; Bierkamp et al., 1996), suggesting that β-catenin may be able to partially compensate for the loss of PG in developing heart muscle.

Neuroepithelium, which resides in the headfolds and in the lining of the spinal canal, is dependent upon notochord development in the early embryo. Prior to neural tube closure, this tissue displays prominent desmosomes, which then disappear once the neural tube is formed (Aaku-Saraste et al., 1996). In our E10 wild-type and mutant embryos, notochord formed, as did neuroepithelium, and neural tube closure took place (Fig. 6A-C). However, in the mutant embryos, the neural tube was often collapsed and the neuroepithelium was malformed.

In areas where the wild-type neural tube had not yet closed, prominent neuroepithelial staining was observed with desmosomal markers, including DP, desmogleins and PG (examples shown in Fig. 6D,E). E-cadherin and other markers of adherens junctions were also detected (example in Fig. 6F). In contrast, while adherens junction markers were still detected in *Dsp* mutant neuroepithelium, desmosomal markers were reduced (Fig. 6G-I). Concomitant with the decrease in desmosomal protein expression was a marked disorganization in neuroepithelial tissue. Despite these abnormalities, the morphologically distinct cells characteristic of this tissue (epindymal, mantle and marginal layer cells) were all still found within the disorganized neuroepithelium of the *Dsp*$^{-/-}$ embryo.

The final tissue that we examined which displays prominent desmosomes was the developing skin epithelium. In wild-type embryos, skin epithelium was only one to two layers thick at E10, and the epithelium was loosely adherent to its underlying substratum, owing to the fact that the anchoring hemidesmosomes, composed of specialized integrins, had not yet formed at this stage. However, desmosomes had already begun to develop and, even at this early time, defects were already evident in *Dsp* mutant skin (Fig. 7A,B). Most notably, aggregates of ectodermal cells were seen, suggesting that cells were loosely adherent to each other as well as to the substratum (Fig. 7B, right). Keratin 8, a marker of embryonic ectoderm (Jackson et al., 1981) revealed that the embryonic skin epithelium of *Dsp*$^{-/-}$ embryos formed, but was not intact (compare Fig. 7C with Fig. 7D). The presence of anti K8 staining along the base of the separated epithelium was suggestive that the epithelium may be fragile, causing intracellular rips (for example, in Fig. 7D). *Dsp* mutant ectoderm displayed a reduction in other desmosome-specific markers, including desmoglein 2, and an absence of DP (Fig. 7E-H). Antibody staining for PG and for specific markers of adherens junctions were positive (not shown).

Ultrastructural analyses confirmed the defects in cell-cell adhesion and the gross disorganization of epithelial cells within E10 *Dsp* mutant skin (Fig. 8). In contrast to wild-type epithelium, which showed a uniform layer of epithelial cells with intercellular contacts (frames A and B), mutant skin showed numerous separations between cells, coupled with some signs of cellular debris (frames C and D). As expected from the antibody staining patterns, adherens junctions and desmosomes were appreciable in the wild-type skin at this

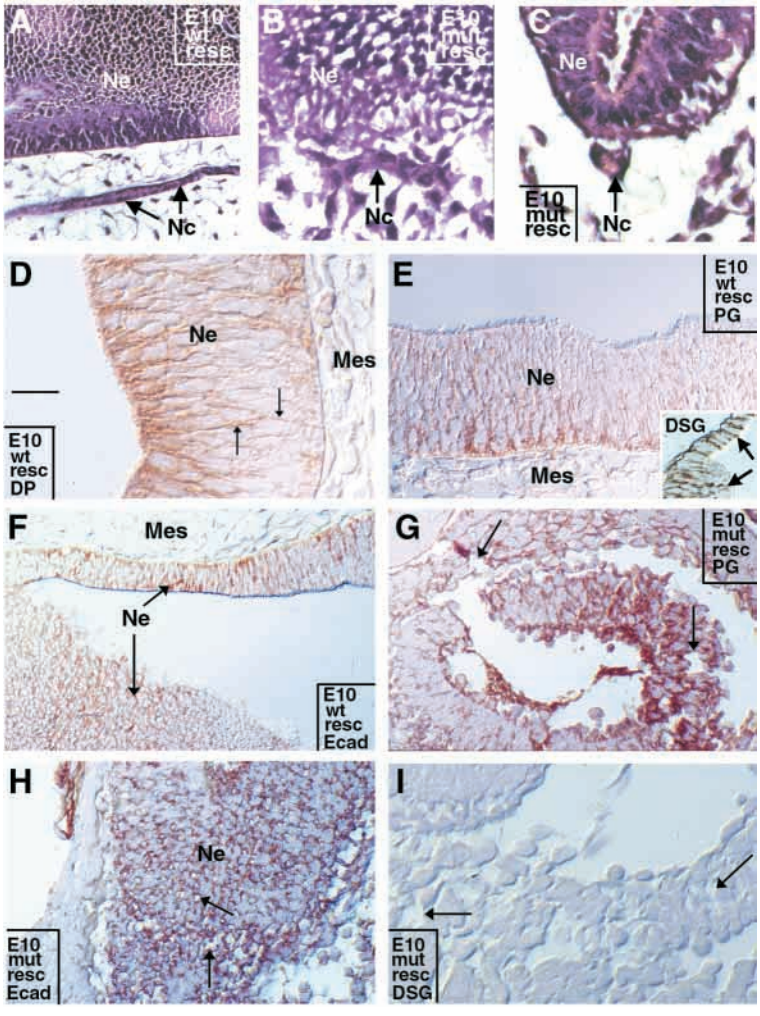

Fig. 6. Perturbations in neuroepithelium in *Dsp*$^{-/-}$ E10 'rescued' embryos. (A-C), Hematoxylin and Eosin-stained sagittal (A,B) and cross (C) sections of E10 wild-type (A) and mutant (B,C) embryos revealing formation of notochord (Nc) and neuroepithelium (Ne). Example in C shows rare area of DP null neural tube that was not collapsed, verifying that formation per se was not affected. Wild-type neuroepithelium (Ne) stained positively for DP (D), PG (E), desmoglein (DSG; inset in E) and E-cadherin. (F) Arrows point to cell junctions. *Dsp*$^{-/-}$ neuroepithelium also stained positively for PG (G) and E-cad (H) but not for DSG (I) or DP (data not shown). Location of Ne in each section was towards anterior region of embryo and prior to neural tube closure. Note distinct spaces between Ne cells in *Dsp*$^{-/-}$ embryos (arrows). Scale bar: 50 μm in B-D,G,I; 100 μm in A,E,F,H.

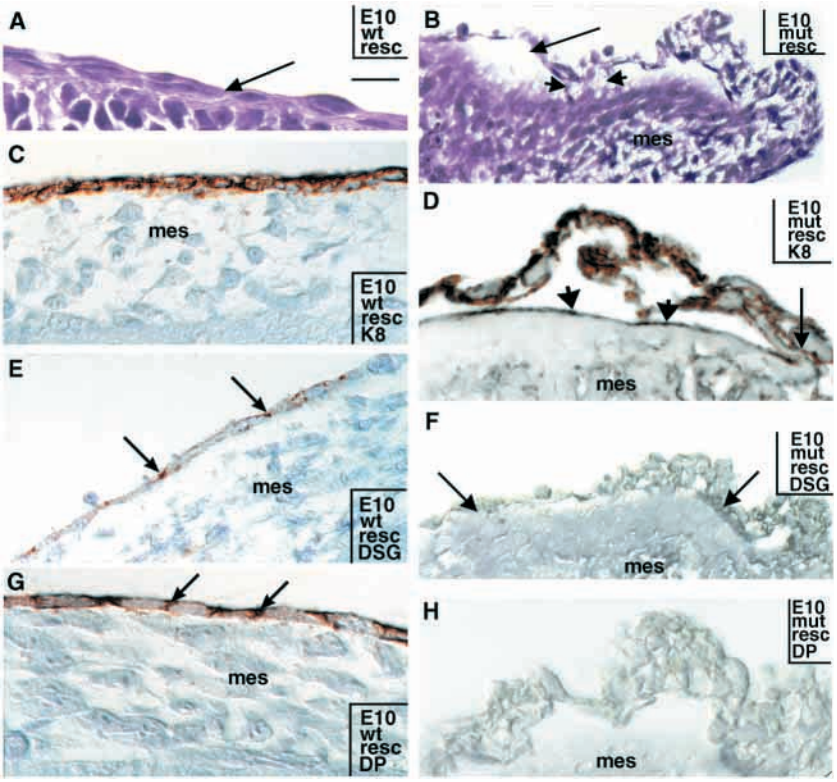

Fig. 7. Skin epithelium of E10 wild-type and *Dsp*$^{-/-}$ 'rescued' embryos. (A,B) Hematoxylin and Eosin staining. Note adherence of wild-type but not *Dsp*$^{-/-}$ surface ectoderm (arrows). Note distinct spaces between *Dsp*$^{-/-}$ ectodermal cells, which are often round. (C,D) Antibodies to keratin 8 stained surface ectoderm in wild-type rescued embryos. Arrow in D points to an area of *Dsp*$^{-/-}$ ectoderm that remained attached to the embryo. Also observed were areas of keratin 8-positive remnants of cells adhered to the basement membrane suggesting possibility that ectodermal cell rupturing may occur upon mild mechanical stress, contributing to detachment of tissue from underlying mesenchyme. (E,F) Anti desmoglein (DSG) staining; (G,H) anti-DP staining. mes, mesoderm. Scale bar: 10 μm in A; 30 μm in B-H.

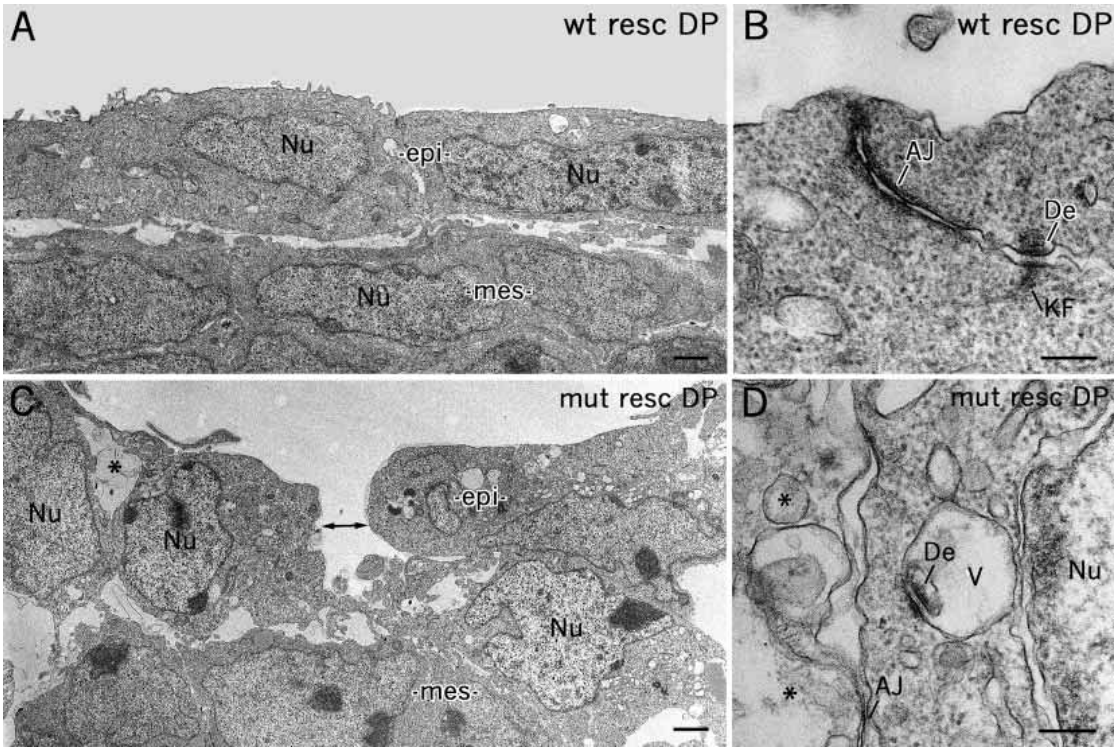

Fig. 8. Ultrastructural analyses of skin epithelium of E10 wild-type and *Dsp*$^{-/-}$ 'rescued' embryos. Wild-type surface ectoderm cells form a single layer of flattened cells connected by adherens junctions and desmosomes (A-D). In *Dsp*$^{-/-}$ embryos, ectodermal cells often appeared round and separated from each other (double arrow in C), with an overall reduction in cell-cell adhesion. Cytoplasmic vacuoles were frequently seen in the null embryonic ectoderm (asterisks). In rare cases where desmosomes could be found in these cells, the desmosomes seemed to reside inside vacuoles (D). Although these desmosomes display typical midlines and outer plaques, the inner plaques were missing, and no attachment to keratin filaments was detected. AJ, adherens junctions; De, desmosomes; epi, developing epidermis; KF, keratin filaments; mes, mesoderm; Nu, nucleus; V, vacuole. Scale bars: 1 μm in A,C; 200 nm in B,D.

stage, and desmosomes were clearly attached to keratin filaments (frame B). In contrast, cell-cell contacts were dramatically perturbed in mutant embryonic skin (frame D). Desmosomes were rare and lacked keratin filament attachments. The presence of cell debris and the paucity of desmosomes in *Dsp* mutant rescued skin is consistent with the knowledge that loss of desmosomes in postnatal skin blistering disorders leads to dissociation of cells within the skin epithelium (for a review, see Kowalczyk et al., 1999). Overall, the defects occurred much earlier in *Dsp* mutant skin development than those observed in PG knockout animals that survived until birth. In the PG knockout skin, a stratified, differentiated epidermis was nearly fully developed before perturbations became evident (Bierkamp et al., 1999).

We wondered whether the desmosomal defects seen in the heart muscle, neuroepithelium or skin epithelium might trigger the programmed cell death machinery and/or cause changes in the proliferative status of the tissues. No significant differences were detected between wild-type and *Dsp* mutant frozen tissue sections that were subjected to TUNEL assays. However, BrdU incorporation was lowered by approximately 25% in all E10 tissues (data not shown). Both desmosomal and non-desmosomal tissues were affected, perhaps a reflection of the poor circulation of the developing animals. Overall, while the dissociation of the tissues reduced proliferation, it did not appear to trigger apoptosis.

Dsp$^{-/-}$ embryos lack well-defined capillaries

Given that DP is a component of the complexus adherens junctions of capillaries (Schmelz and Franke, 1993; Schmelz et al., 1994), we examined the vasculature of DP null embryos (Fig. 9). In contrast to wild-type E10 embryos, which displayed a well-formed capillary network (Fig. 9A), the number of capillaries in mutant embryos was significantly reduced (Fig. 9B). Thus, whereas wild-type E10 embryos contained 43±5 capillaries per sagittal section, *Dsp* mutant embryos showed only, 7±1 capillaries per section. The endothelial lining of many of the *Dsp*$^{-/-}$ capillaries also exhibited distinct disruptions not observed in capillaries of wild-type embryos (arrows in Fig. 9A,B). In some sections, blood cells were scattered in the surrounding areas (Fig. 9B). Larger blood vessels (those greater than one blood cell in diameter), however, appeared normal (arrowheads in Fig. 9B). This finding was consistent with the fact that DP is a component of capillaries but not blood vessels (Schmelz et al., 1994; Kowalczyk et al., 1998).

Indirect immunofluoresence using markers to capillaries was used to confirm their identity in embryo sections. Antibodies to vimentin, VEGF, VE-Cadherin, CD-34 and PG all defined the boundaries of each capillary (representative wild-type examples in Figs 9C,D,F). As judged by immunostaining with these antibodies, all revealed fewer capillaries per section in *Dsp*$^{-/-}$ embryos when compared with wild-type embryos (Figs 9E,G). Furthermore, while VE-cadherin, PG and vimentin staining persisted in capillaries of *Dsp*$^{-/-}$ embryos, few well-defined capillary walls were present.

Dsp$^{-/-}$ embryoid bodies are not efficient at producing capillary-like structures

A priori, the severe defects in the developing heart of *Dsp* mutant embryos could account for the reduction in capillaries. An equally plausible explanation, however, is that, without DP, endothelial cells of the capillary are weakened in their attachments, because they are unable to form complexus adherens junctions. To attempt to distinguish between these possibilities, we took advantage of the fact that wild-type, ES cell-derived embryoid bodies (EBs) can be manipulated in culture to form endothelial chords that possess typical endothelial cell-cell junctions resembling those of capillaries (Wang et al., 1992; Vittet et al., 1996; Vittet et al., 1997).

Two *Dsp*$^{-/-}$ clones were generated from the *Dsp*$^{+/-}$ lines that we had used for our previous study (Gallicano et al, 1998). The elevation of neomycin to select for double recombinants was used as a selection procedure (see Mortenson et al., 1992 for details). A *Dsp*$^{+/-}$ ES clone subjected to the same procedure

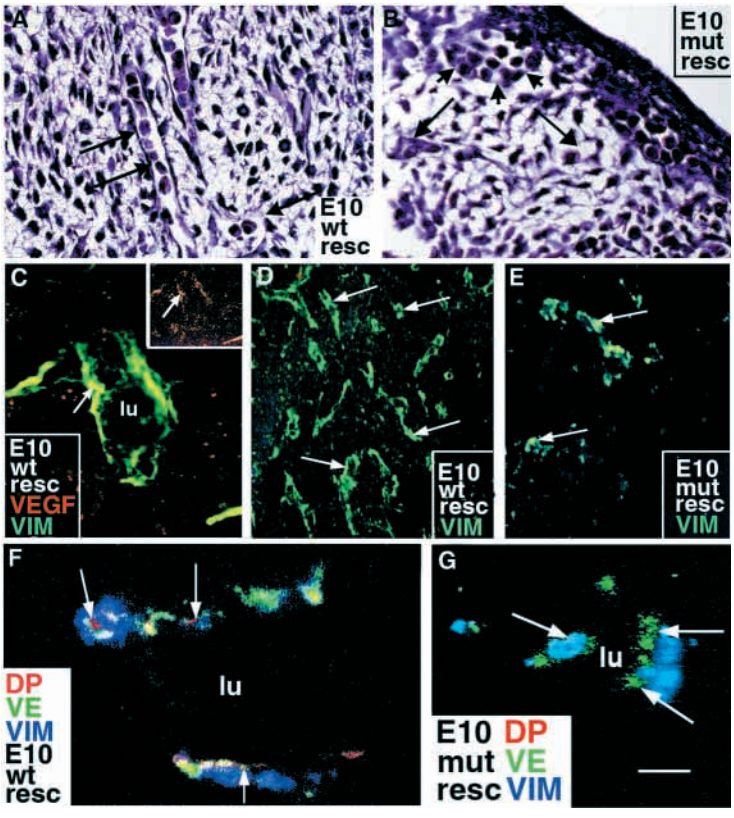

Fig. 9. Analyses of capillaries in wild-type and *Dsp*$^{-/-}$ E10 'rescued' embryos. (A) Hematoxylin and Eosin-stained paraffin- embedded sections of wild-type embryo contained numerous capillaries (arrows) in mesenchyme (shown) and neuroepithelium (not shown). (B) In *Dsp*$^{-/-}$ embryos, well-developed capillaries were not easily detected. Capillaries that were present usually were disrupted (arrows) and in some instances, blood cells escaped from the vessel (at tip of right arrow). Large blood vessels (short arrows in B) appeared unaffected. (C-G) High magnification, confocal imaging with antibody markers for capillaries to reveal the endothelial lining of capillaries (arrows) in wild-type (C,D,F) and *Dsp*$^{-/-}$ (E,G) embryos. Antibodies are color coded as indicated in corner of each frame. VE, VE-cadherin; VEGF, vascular endothelial growth factor; VIM, vimentin. Arrows denote capillary-like structures, much reduced in *Dsp*$^{-/-}$ embryos. Scale bar: 100 μm in A,B; 40 μm in C; 250 μm in D,E; 15 μm in F,G.

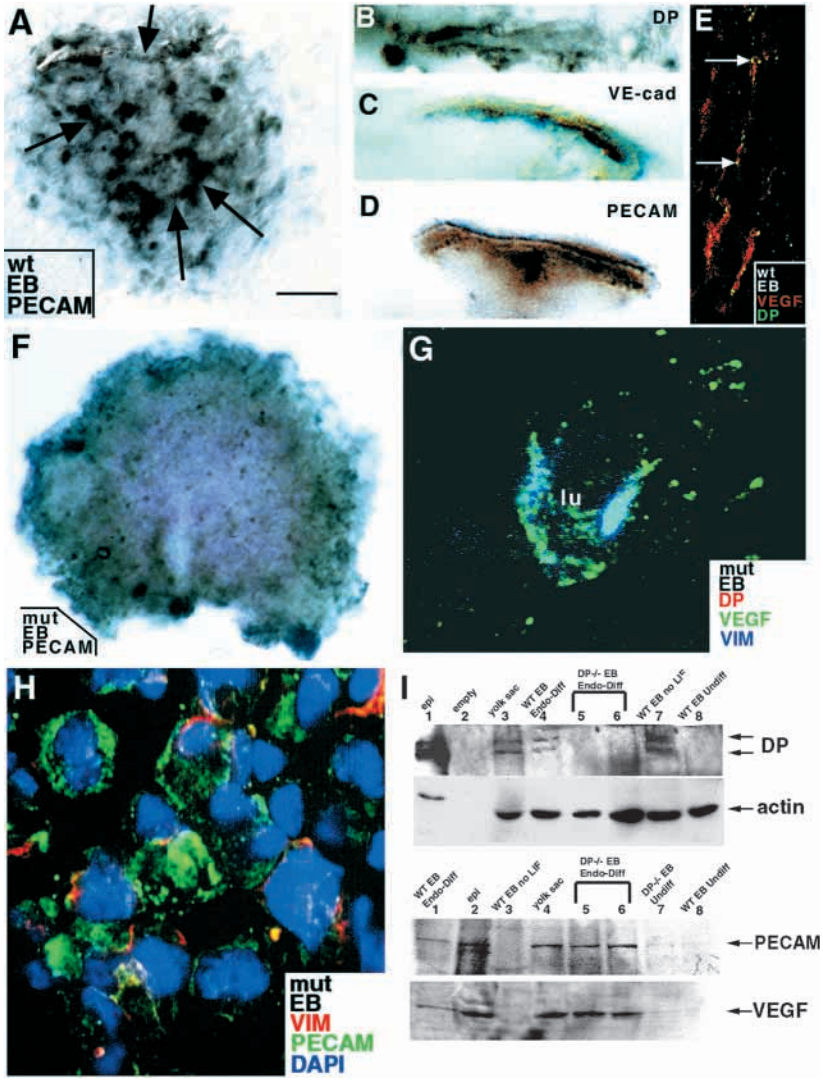

Fig. 10. Cultured wild-type and *Dsp*$^{-/-}$ embryoid bodies (EBs) optimized for endothelial differentiation. (A,F) EBs differentiated for 14 days (see Materials and Methods) and stained with platelet endothelial cell adhesion marker (PECAM) antibodies followed by HRP enhancement. Note PECAM-positive endothelial chords (arrows) in wild type, missing in *Dsp*$^{-/-}$ EB. (B-D) Wild-type EBs were crushed between the slide and coverslip releasing tube-like structures, which stained positively for DP (B), VE-cadherin (C) and PECAM (D). (E) DP antibodies stained endothelial chords in wild-type EBs, which were confirmed using antibodies to VEGF (data not shown). (G) The few endothelial chords that were found in *Dsp*$^{-/-}$ EBs stained positive for vimentin (blue) and VEGF (green). (H) Most *Dsp*$^{-/-}$ EBs stained with antibodies to PECAM and vimentin showed clumps of endothelial cells positive for these proteins, but no endothelial chords (high magnification view). (I) *Dsp*$^{-/-}$ and wild-type EBs were immunoblotted with antibodies to DP, actin, PECAM and VEGF. Anti-DP: lane 1, newborn epidermis was positive for both forms of DP; lane 2, empty; lane 3, yolk sac was positive; lane 4, endothelial differentiated wild-type EBs were positive; lane 5, endothelial differentiated *Dsp*$^{-/-}$ EB clone 1 was negative for DP; lane 6, endothelial differentiated *Dsp*$^{-/-}$ EB clone 2 was negative for DP; lane 7, wild-type EBs differentiated without LIF and without endothelial differentiation components were positive for DP; lane 8, undifferentiated wild-type EBs (14 days in culture with LIF) were negative for DP. Anti-actin (same blot as in D, except stripped and probed with actin antibodies to show loading). Anti-PECAM: lane 1, wild-type EBs endothelial differentiated were positive; lane, 2 newborn skin was positive; lane 3, wild-type EBs without endothelial differentiation components were negative; lane 4, yolk sac was positive; lane 5, endothelial differentiated *Dsp*$^{-/-}$ EB clone 1 was positive; lane 6, endothelial differentiated *Dsp*$^{-/-}$ clone 2 was positive; lane 7, *Dsp*$^{-/-}$ EBs incubated without LIF and without endothelial differentiation components was slightly positive; lane 8, undifferentiated wild-type EB (14 days in culture with LIF) was slightly positive. Anti-VEGF: blot F was stripped and reprobed with antibodies against VEGF. The same lanes that were positive for PECAM were also positive for VEGF. Scale bar: 175 μm in A,F; 100 μm in B-D; 25 μm in G; 15 μm in H.

was used as a positive control to verify that the effects observed were not due to the selection method. In the assays to follow, the *Dsp*$^{+/-}$ clone behaved analogously to the wild-type *Dsp*$^{+/+}$ controls and both *Dsp*$^{-/-}$ clones behaved comparably.

Under the correct culture conditions (see Materials and Methods), *Dsp*$^{+/+}$, *Dsp*$^{+/-}$ and *Dsp*$^{-/-}$ embryoid bodies were grown for 11-14 days in culture followed by immunohistochemistry with antibodies against endothelial cell markers. Antibodies against platelet endothelial cell adhesion marker (PECAM), a known endothelial adhesion protein, was used to stain the distinct endothelial chords that formed in *Dsp*$^{+/+}$ and *Dsp*$^{+/-}$ differentiated EBs (Fig. 10A). ES cells allowed to differentiate by incubation in normal media but without LIF did not exhibit these endothelial chords as judged by the absence of labeled structures (data not shown). At higher magnification and using a variety of capillary marker antibodies, the capillary-like nature of these chords was evident (Fig. 10B-E).

Overall, the microvasculature induced in wild-type EBs resembled the capillary network found in vivo. This included expression of all of the complexus adherens junction markers. In contrast, when either of our two *Dsp*$^{-/-}$ ES clones were cultured under conditions optimal for endothelial chord differentiation, they did not form discernable chords as judged by immunohistochemistry with antibodies against PECAM (Fig. 10F). Differentiated *Dsp*$^{-/-}$ EBs did contain a few short VEGF- and vimentin-positive chord-like structures (Fig. 10G), as well as some vimentin-positive, PECAM-positive cells (Fig. 10H), indicating that the cultures were able to differentiate into endothelial cells in the absence of DP. Immunoblot analyses confirmed the presence of endothelial markers in the *Dsp*$^{-/-}$ differentiated cultures (Fig. 10I). However, without DP, endothelial cells were found mostly as aggregates instead of well-developed chord-like structures (Fig. 10H). Based on these data, it appeared that, without DP, endothelial cells formed, but were not able to assemble into capillary-like tubes.

DISCUSSION

Previously it has been shown that DP is essential for early mammalian development since its ablation led to early embryonic lethality at E6.5 (Gallicano et al., 1998). During development, DP exhibits at least two functions: (1) anchoring and maintaining an anastomosing network of keratin intermediate filaments to desmosomes; and (2) assembling and/or stabilizing desmosomes (Gallicano et al., 1998). Although these general functions of DP were revealed from our earlier study, determining the role of DP in somatic tissues was not possible without rescuing the DP-related defects in the extra-embryonic tissues of the embryos. From our current study, a common theme that has emerged is that, without DP, the three-dimensional architecture of many developing tissues is severely compromised without affecting cell differentiation or the spatiotemporal pattern of developing tissues and organs.

One of the first organs to form in mammals is the heart. In wild-type embryos at about E7.5-E8.0, distinct mesodermal cells form bilateral cardiac progenitor cells that fuse and form a primitive heart tube (Arai et al., 1997). Distinctive beating of the developing heart begins at about E8.5, after which blood begins to pump through the heart tube and into other tissues of the developing embryo. As blood pressure rises, stress increases in cardiac cells resulting in a need for intercellular junctions, e.g. desmosomes, strong enough to compensate for such increases. DP, essential both for anchorage to IFs and for either desmosome formation or stability (Gallicano et al, 1998), is expressed early in the heart anlage (van der Loop et al., 1995) where it and other desmosomal components assemble into myocardial cell adhesion junctions known as intercalated disks (Franke et al., 1982; Kartenbeck et al, 1983).

While PG and DP are both components of the desmosomes of the intercalated disks of the developing heart, the severity in the *Dsp* mutant embryos appeared to be considerably greater than in the PG mutant animals of seemingly comparable genetic background (compare this report with that of Ruiz et al., 1996; Bierkamp et al., 1996; Isac et al., 1999). Thus, some PG null animals survived until birth, while all of the *Dsp* mutant animals that we examined exhibited severe heart defects and died by E10. The most likely explanation for this difference resides in the ability of β-catenin to at least partially compensate for the function of PG in heart muscle desmosomes. In this regard, Ruiz et al. found a novel amalgamated junction, composed of DP and β-catenin, but not desmosomal cadherins, in the PG knockout heart muscle (Ruiz et al., 1996), while Bierkamp et al. found that in the skin of these embryos, desmosomes still formed, but they were composed of β-catenin, apparently acting as a substitute for PG (Bierkamp et al., 1999). When taken together with our study here, partially compensatory mechanisms for PG and β-catenin would explain the late onset of heart defects in the PG null animals.

In contrast to PG, DP appears to have no compensatory counterpart. Thus, the loss of DP compromised cardiac output shortly after gastrulation and resulted in a collapsed heart. Despite these severe abnormalities in tissue integrity, the endocardium, myocardium and epicardium still formed and were spatially oriented in the proper fashion in DP null embryos suggesting that DP, like PG, did not play a significant role in heart tissue differentiation.

Another marked abnormality in $Dsp^{-/-}$ embryos was their inability to form proper head folds and spinal canal. These structures are a product of embryonic ectoderm. By E7.5, anterior ectoderm begins to form a sheet of cells displaying distinct polarity, complete with tight, adherens and desmosomal junctions (Miragall and Mendoza, 1982; Aaku-Saraste et al., 1996; Kowalczyk et al., 1999). These ectodermal cells form the neuroepithelium, which persists until about E11 when neurogenesis occurs and the cells differentiate into distinct neurons (Bally-Cuif et al., 1993; Aaku-Saraste et al., 1996). Desmosomes are abundant in the neuroepithelium, but after the neural tube begins to form at about E8.5, epithelial gene expression is replaced by neural gene expression (Aaku-Saraste et al., 1996). Our study here provides the first indication that DP and desmosomes are essential for neuroepithelial adhesion and for complete neural tube closure. Again, similar to our findings regarding the role of DP in cardiac development, differentiation of neuroepithelium seemed unaffected in *Dsp* mutant embryos. Rather, the loss of DP appeared to prevent neuroepithelium from undergoing and/or stabilizing neural tube formation. In this regard, the DP-induced defect in the neuroepithelium resembled the failure of egg cylinder expansion caused by the lack of DP in visceral endoderm (Gallicano et al., 1998).

The final desmosomal-containing tissue that was clearly perturbed in *Dsp* mutant embryos was the developing skin epithelium. Desmosomes can be found in this tissue shortly after gastrulation (Weiss and Zellickson, 1975). However, in the PG knockout, skin epithelial abnormalities did not appear until approx. E17.5 (Bierkamp et al., 1996; Bierkamp et al., 1999), leaving the role of desmosomes in early embryonic skin development undetermined. Our study reveals a role for DP in skin epithelium as early as desmosomes begin to form in this tissue.

In contrast to the PG knockout (Ruiz et al, 1996; Bierkamp et al, 1996), desmocollin levels appeared to be significantly perturbed in the early developing DP null skin. Thus, whereas PG cousins, such as plakophilins or β-catenin, seem to compensate functionally for PG in developing skin epithelium (Bierkamp et al., 1999), DP does not appear to have such compensatory proteins, enabling us to conclude that desmosomes play a crucial role in epithelial tissue integrity in the developing skin long before the embryo is subjected to the major mechanical stresses of moving through the birth canal. Our results are interesting in light of a recent report that haploinsufficiency of DP can lead to a blistering disorder in humans (Armstrong et al., 1999; Whittock et al., 1999) and extend a role for DP to embryonic skin. Taken together, our findings provide strong evidence that DP is essential for desmosome stability and mechanical integrity in developing epidermis as we had shown previously for extra-embryonic ectoderm.

We were intrigued by the fact that markedly fewer capillaries were found in *Dsp* mutant embryos than in wild-type animals. A priori, this could be a secondary consequence of the dramatically reduced cardiac output seen in these embryos. While capillary defects were not noted in the PG null embryos (Bierkamp et al., 1996; Ruiz et al., 1996), we cannot rule out the possibility that the relatively late onset of heart failure in the PG null animals bypasses the window of capillary development and consequently has no effect on the process. A

more intriguing alternative explanation, however, is that capillary integrity is compromised in the *Dsp* mutant embryos as a direct consequence of the ablation of DP in the developing capillaries. We favor this hypothesis, given the fact that two independently derived clones of ES cells failed to form endothelial chords that resemble capillaries. In contrast, our ES wild-type cultures readily formed these structures under the conditions we used for differentiation (Vittet et al., 1997). Additionally, it is notable that large blood vessels that do not express DP (Schmelz and Franke, 1993; Schmelz et al., 1994) appeared unaffected in the DP null embryos.

The paucity of capillaries in $Dsp^{-/-}$ embryos was intriguing in that a similar abnormality was observed in E9.5 embryos deficient for VE-cadherin (Carmeliat et al., 1999). In that study, it was shown that mutated versions of VE-cadherin did not disrupt endothelial formation of small blood vessels, but impaired their remodeling and maturation leading to embryonic lethality at E9.5. Our findings suggest that the loss of DP causes a similar weakening of endothelial cell adhesion, leading to a marked defect in capillary formation.

In summary, by using the tetraploid aggregation assay to rescue $Dsp^{-/-}$ embryos that normally die at E6.5, new insights into the function of DP and desmosomes during organogenesis have been uncovered. Compromised in $Dsp^{-/-}$-rescued embryos is the structural integrity of tissues that normally contain desmosomes or complexus adherens junctions and that undergo some type of mechanical stress or dynamic change in organization. Interestingly, these defects were often manifested in a failure of tube formation, e.g. the egg cylinder, the spinal canal and capillaries. Taken together, these findings suggest that DP functions not only in desmosome stability but also in the formation of complexus adherens junctions. Presumably, without crucial stability of these junctions and their anchorage to IFs, mechanical strength of intercellular adhesion is compromised. More detailed analysis of the precise role of DP in the structure and assembly of desmosomes and complexus adherens junctions must await the engineering of later stage, tissue-specific knockouts of *Dsp*. These will be needed for establishment of pure populations of DP null endothelial or epidermal cultures.

We thank Dr Werner Franke for his kind gift of desmosomal antibodies used in these studies. We also thank Dr Helene Baribault for her generosity and expert training given in tetraploid aggregation and embryo rescue. This work was supported by funds from the National Institutes of Health (R01-AR27883). The mouse studies were carried out in the University of Chicago transgenic and embryonic stem cell facility, subsidized by a grant from the National Cancer Institute. E. F. is an Investigator of the Howard Hughes Medical Institute.

REFERENCES

Allen, E., Yu, Q. C. and Fuchs, E. (1996). Mice expressing a mutant desmosomal cadherin exhibit abnormalities in desmosomes, proliferation, and epidermal differentiation. *J. Cell Biol.* **133**, 1367-1382.

Aaku-Saraste, E., Hellwig, A. and Huttner, W. B. (1996). Loss of occludin and functional tight junctions, but not ZO-1, during neural tube closure–remodeling of the neuroepithelium prior to neurogenesis. *Dev. Biol.* **180**, 664-679.

Arai, A., Yamamoto, K. and Toyama, J. (1997). Murine cardiac progenitor cells require visceral embryonic endoderm and primitive streak for terminal differentiation. *Dev. Dyn.* **210**, 344-353.

Armstrong, D. K., McKenna, K. E., Purkis, P. E., Green, K. J., Eady, R. A., Leigh, I. M. and Hughes, A. E. (1999). Haploinsufficiency of desmoplakin causes a striate subtype of palmoplantar keratoderma. *Hum. Mol. Genet.* **8**, 143-148.

Bally-Cuif, L., Goridis, C. and Santoni, M. J. (1993). The mouse NCAM gene displays a biphasic expression pattern during neural tube development. *Development* **117**, 543-552.

Barth, A. I., Nathke, I. S. and Nelson, W. J. (1997). Cadherins, catenins and APC protein: interplay between cytoskeletal complexes and signaling pathways. *Curr. Opin. Cell Biol.* **9**, 683-690.

Bierkamp, C., Mclaughlin, K. J., Schwarz, H., Huber, O. and Kemler, R. (1996). Embryonic heart and skin defects in mice lacking plakoglobin. *Dev. Biol.* **180**, 780-785.

Bierkamp, C., Schwarz, H., Huber, O. and Kemler, R. (1999). Desmosomal localization of beta- catenin in the skin of plakoglobin null-mutant mice. *Development* **126**, 371-381.

Carmeliet, P., Lampugnani, M. G., Moons, L., Breviario, F., Compernolle, V., Bono, F., Balconi, G., Spagnuolo, R., Oostuyse, B., Dewerchin, M. et al. (1999). Targeted deficiency or cytosolic truncation of the VE-cadherin gene in mice impairs VEGF-mediated endothelial survival and angiogenesis. *Cell* **98**, 147-157.

Cowin, P., Kapprell, H.-P., Franke, W. W., Tamkun, J. and Hynes, R. O. (1986). Plakoglobin: a protein common to different kinds of intercellular adhering junctions. *Cell* **47**, 1063-1073.

Dragatsis, I., Efstratiadis, A. and Zeitlin, S. (1998). Mouse mutant embryos lacking huntingtin are rescued from lethality by wild-type extraembryonic tissues. *Development* **125**, 1529-1539.

Drake, C. J. and Fleming, P. A. (2000). Vasculogenesis in the day 6.5 to 9.5 mouse embryo. *Blood* **95**, 1671-1679.

Duncan, S. A., Nagy, A. and Chan, W. (1997). Murine gastrulation requires HNF-4 regulated gene expression in the visceral endoderm: tetraploid rescue of $Hnf\text{-}4^{-/-}$ embryos. *Development* **124**, 279-287.

Franke, W. W., Grund, C., Kuhn, C., Jackson, B. W. and Illmensee, K. (1982). Formation of cytoskeletal elements during mouse embryogenesis. III. Primary mesenchymal cells and the first appearance of vimentin filaments. *Differentiation* **23**, 43-59.

Gallicano, G. I. and Capco, D. G. (1995). Remodeling of the specialized intermediate filament network in mammalian eggs and embryos during development: regulation by protein kinase C and protein kinase M. *Curr. Top. Dev. Biol.* **31**, 277-320.

Gallicano, G. I., Kouklis, P., Bauer, C., Yin, M., Vasioukhin, V., Degenstein, L. and Fuchs, E. (1998). Desmoplakin is required early in development for assembly of desmosomes and cytoskeletal linkage. *J. Cell Biol.* **143**, 2009-2022.

Hogan, B., Beddington, R., Constantini, F. and Lacy, E. (1994). *Manipulating the mouse embryo.* Cold Spring Harbor, NY: Cold Spring Harbor Laboratory Press.

Isac, C. M., Ruiz, P., Pfitzmaier, B., Haase, H., Birchmeier, W. and Morano, I. (1999). Plakoglobin is essential for myocardial compliance but dispensable for myofibril insertion into adherens junctions. *J. Cell Biochem.* **72**, 8-15.

Jackson, B. W., Grund, C., Winter, S., Franke, W. W. and Illmensee, K. (1981). Formation of cytoskeletal elements during mouse embryogenesis. II. Epithelial differentiation and intermediate-sized filaments in early postimplantation embryos. *Differentiation* **20**, 203-216.

Jollie, W. P. (1990). Development, morphology, and function of the yolk-sac placenta of laboratory rodents. *Teratology* **41**, 361-381.

Kadokawa, Y., Kato, Y. and Eguchi, G. (1987). Cell lineage analysis of the primitive and visceral endoderm of mouse embryos cultured in vitro. *Cell Differ.* **21**, 69-76.

Kartenbeck, J., Franke, W. W., Moser, J. G. and Stoffels, U. (1983). Specific attachment of desmin filaments to desmosomal plaques in cardiac myocytes. *EMBO J.* **2**, 735-742.

Kaufman, M. H. (1992). *The Atlas of Mouse Development.* New York: Academic Press.

Koch, P. J. and Franke, W. W. (1994). Desmosomal cadherins: another growing multigene family of adhesion molecules. *Curr. Opin. Cell Biol.* **6**, 682-687.

Kouklis, P., Hutton, E. and Fuchs, E. (1994). Making the connection: keratin intermediate filaments and desmosomes proteins. *J. Cell Biol.* **127**, 1049-1060.

Kowalczyk, A. P., Bornslaeger, E. A., Borgwardt, J. E., Palka, H. L., Dhaliwal, A. S., Corcoran, C. M., Denning, M. F. and Green, K. J. (1997). The amino-terminal domain of desmoplakin binds to plakoglobin

and clusters desmosomal cadherin-plakoglobin complexes. *J. Cell Biol.* **139**, 773-784.

Kowalczyk, A. P., Navarro, P., Dejana, E., Bornslaeger, E. A., Green, K. J., Kopp, D. S. and Borgwardt, J. E. (1998). VE-cadherin and desmoplakin are assembled into dermal microvascular endothelial intercellular junctions: a pivotal role for plakoglobin in the recruitment of desmoplakin to intercellular junctions. *J. Cell Sci.* **111**, 3045-3057.

Kowalczyk, A. P., Bornslaeger, E. A., Norvell, S. M., Palka, H. L. and Green, K. J. (1999). Desmosomes: intercellular adhesive junctions specialized for attachment of intermediate filaments. *Int. Rev. Cytol.* **185**, 237-302.

Kupriyanov, S. and Baribault, H. (1998). Genetic control of extraembryonic cell lineages studied with tetraploid<–>diploid chimeric concepti. *Biochem. Cell Biol.* **76**, 1017-1027.

Lampugnani, M. G. and Dejana, E. (1997). Interendothelial junctions: structure, signalling and functional roles. *Curr. Opin. Cell Biol.* **9**, 674-682.

McGrath, J. A., McMillan, J. R., Shemanko, C. S., Runswick, S. K., Leigh, I. M., Lane, E. B., Garrod, D. R. and Eady, R. A. J. (1997). Mutations in the plakophilin 1 gene result in ectodermal dysplasia/skin fragility syndrome. *Nature Genet.* **17**, 240-244.

Mertens, C., Kuhn, C. and Franke, W. W. (1996). Plakophilins 2a and 2b:constitutive proteins of dual location in the karyoplasm and the desmosomal plaque. *J. Cell Biol.* **135**, 1009-1025.

Miragall, F. and Mendoza, A. S. (1982). Intercellular junctions in the rat vomeronasal neuroepithelium: a freeze-fracture study. *J. Submicrosc. Cytol.* **14**, 597-605.

Mortensen, R. M., Conner, D. A., Chao, S., Geisterfer-Lowrance, A. A. and Seidman, J. G. (1992). Production of homozygous mutant ES cells with a single targeting construct. *Mol. Cell Biol.* **12**, 2391-2395.

Nagy, A., Rossant, J., Nagy, R., Abramow-Newerly, W. and Roder, J. C. (1993). Derivation of completely cell culture-derived mice from early-passage embryonic stem cells. *Proc. Natl. Acad. Sci. USA* **90**, 8424-8428.

Ruiz, P., Brinkmann, V., Ledermann, B., Behrend, M., Grund, C., Thalhammer, C., Vogel, F., Birchmeier, C., Gunthert, U., Franke, W. W. and Birchmeier, W. (1996). Targeted mutation of plakoglobin in mice reveals essential functions of desmosomes in the embryonic heart. *J. Cell Biol.* **135**, 215-225.

Schmelz, M. and Franke, W. W. (1993). Complexus adhaerentes, a new group of desmoplakin-containing junctions in endothelial cells: the syndesmos connecting retothelial cells of lymph nodes. *Eur. J. Cell Biol.* **61**, 274-289.

Schmelz, M., Moll, R., Kuhn, C. and Franke, W. W. (1994). Complexus adhaerentes, a new group of desmoplakin-containing junctions in endothelial cells: II. Different types of lymphatic vessels. *Differentiation* **57**, 97-117.

Schwarz, S. M., Gallicano, G. I., McGaughey, R. W. and Capco, D. G. (1995). A role for intermediate filaments in the establishment of the primitive epithelia during mammalian embryogenesis. *Mech. Dev.* **53**, 305-321.

Smith, E. and Fuchs, E. (1998). Defining the interactions between intermediate filaments and desmosomes. *J. Cell Biol.* **141**, 1229-1241.

Stappenbeck, T. S., Bornslaeger, E. A., Corcoran, C. M., Luu, H. H., Virata, M. L. and Green, K. J. (1993). Functional analysis of desmoplakin domains: specification of the interaction with keratin versus vimentin intermediate filament networks. *J. Cell Biol.* **123**, 691-705.

Stappenbeck, T. S. and Green, K. J. (1992). The desmoplakin carboxyl terminus coaligns with and specifically disrupts intermediate filament networks when expressed in cultured cells. *J. Cell Biol.* **116**, 1197-1209.

Sulik, K., Dehart, D. B., Iangaki, T., Carson, J. L., Vrablic, T., Gesteland, K. and Schoenwolf, G. C. (1994). Morphogenesis of the murine node and notochordal plate. *Dev. Dyn.* **201**, 260-278.

van der Loop, F. T., Schaart, G., Langmann, H., Ramaekers, F. C. and Viebahn, C. (1995). Rearrangement of intercellular junctions and cytoskeletal proteins during rabbit myocardium development. *Eur. J. Cell Biol.* **68**, 62-69.

Vittet, D., Prandini, M. H., Berthier, R., Schweitzer, A., Martin-Sisteron, H., Uzan, G. and Dejana, E. (1996). Embryonic stem cells differentiate in vitro to endothelial cells through successive maturation steps. *Blood* **88**, 3424-3431.

Vittet, D., Buchou, T., Schweitzer, A., Dejana, E. and P. H. (1997). Targeted null-mutation in the vascular endothelial-cadherin gene impairs the organization of vascular-like structures in embryoid bodies. *Proc. Natl. Acad. Sci. USA* **94**, 6273-6278.

Wang, R., Clark, R. and Bautch, V. L. (1992). Embryonic stem cell-derived cystic embryoid bodies form vascular channels: an in vitro model of blood vessel development. *Development* **114**, 303-316.

Weiss, L. W. and Zelickson, A. S. (1975). Embryology of the epidermis: ultrastructural aspects. *Acta Dermato-Venereologica* **55**, 161-168.

Whittock, N. V., Ashton, G. H., Dopping-Hepenstal, P. J., Gratian, M. J., Keane, F. M., Eady, R. A. and McGrath, J. A. (1999). Striate palmoplantar keratoderma resulting from desmoplakin haploinsufficiency. *J. Invest. Dermatol.* **113**, 940-946.